Radiation Physics and Chemistry 236 (2025) 112880

Contents lists available at ScienceDirect

Radiation Physics and Chemistry

journal homepage: www.elsevier.com/locate/radphyschem

Characterization of a 1.5 MeV electron beam irradiator using a homemade diode-based dosimetry system

J.A.C. Gonçalves [a], V.K. Asfora [b], H.J. Khoury [b], C.C. Bueno [a,*]

[a] Instituto de Pesquisas Energéticas e Nucleares, 05508-000, São Paulo, SP, Brazil
[b] Depto. de Energia Nuclear - Universidade Federal de Pernambuco, 50740-545, Recife, PE, Brazil

ARTICLE INFO

Handling editor: Chris Chantler

Keywords:
Electron beam processing dosimetry
Si PIN photodiode
Electron beam profile
Electron dosimetry

ABSTRACT

The characterization of an industrial-scale electron beam irradiator using an online diode-based dosimetry system, previously developed and calibrated for routine processes control, is presented in this work. The investigation is focused on the dose per pass and beam length operating parameters of the EB facility, which most take advantage of the online dosimetry performance based on an unbiased diode with linear dose response and stable current signal proportional to the dose rate. The dose per pass values are obtained through integrating the current signals delivered by the diode irradiated at a constant dose rate (4 kGy/s) under (2–6 m/min) conveyor speeds. The integration time of the electrometer on the current signal shape is also investigated from 0.05 to 0.55 s. All dose per pass results perfectly match those assessed with reference standard alanine dosimeters, regardless of the integration time. However, the most precise dose per pass data, quantified through the lowest residues to the alanine measurements, is obtained at 0.1 s, where Gaussian current signals with well-defined centroid and FWHM parameters are achieved. It enables applying the straightforward method to assess the beam length through a current signal, provided it realistic traduces the dose rate variations as a function of the time while the diode passes through the beam. The validity of this approach is checked by measuring the beam length at 4 kGy/s, 6 m/min speed conveyor, and 17 cm from the scan window, which are the conditions mostly used in routine processes conducted in this EB facility. A good agreement is found among the FWHM of beam profiles, assessed with the diode (9.7 cm), CTA film (6.6 cm), a standard dosimeter for this type of measurement, and alanine dosimeters (7.1 cm). The differences between the spatial resolution of the dosimeters perfectly justify the small discrepancies found in the FWHM values.

It is noteworthy that the overall results presented herein, benchmarked against those assessed with reference standard passive dosimeters for radiation processing dosimetry, not only validate the approach to measure the dose per pass and beam length parameters, but also endorses the reliable performance of this diode-based system as an inexpensive and reliable dosimeter for routine process control.

1. Introduction

Electron beam (EB) irradiators have been widely used for radiation processing applications encompassing high absorbed doses (10–100 kGy) and ultra-high dose rates (kGy/s) (Cleland et al., 2003; Cleland, 2006; ICRU-Report 80, 2008; Calvo et al., 2012; IAEA TECDOC-2008, 2022). For such applications, the major consideration in designing the EB accelerator is to achieve a uniform absorbed dose distribution in the irradiated product with efficient utilization of the electron energy and the cost-effectiveness of the process (Cleland et al., 1993; Galloway et al., 2004a; 2004b). Accurate dosimetry is essential to ensure the reliability of the whole process, and several well-established dosimeters (graphite calorimeter, alanine, cellulose triacetate) are available for EB processing dosimetry (McLaughlin et al., 1989; Chilkulwar et al., 2012; ISO/ASTM 52628, 2013; ISO/ASTM 51650, 2013; ISO/ASTM 51649, 2015). However, variations in the electron energy, beam profiles, attainable dose rate, and conveyor speed also affect the dose absorbed in the irradiated product, requiring constant control and monitoring of these parameters (Farah et al., 2004; Benny et al., 2014). Following the international standard recommendations, this task is accomplished in

This article is part of a special issue entitled: ISRP-16 published in Radiation Physics and Chemistry.

* Corresponding author.
E-mail address: ccbueno@ipen.br (C.C. Bueno).

https://doi.org/10.1016/j.radphyschem.2025.112880
Received 20 December 2024; Received in revised form 25 April 2025; Accepted 25 April 2025
Available online 8 May 2025

static irradiation mode with passive dosimeters, mainly by alanine and cellulose triacetate. Although the measurements are accurate, they are time-consuming, which reduces the efficiency of the irradiation process.

Active dosimeters that provide real-time data with stable response are the most suitable for monitoring the process and the accelerator parameters (Barthe, 2001; Smith and Galloway, 2004; Yuan et al., 2023). They might be a useful tool for improving the cost-effectiveness of the entire process, enabling corrective actions to avoid loss of material or unscheduled shutdowns of the accelerator (McLaughlin et al., 1989; Kneeland et al., 1999). These surmises motivated the first attempts to develop active dosimeters based on silicon diodes for process monitoring and mapping fields of high-activity ^{60}Co sources (Muller, 1970a, 1970b; Osvay et al., 1975a, 1975b; Möhlmann, 1981; Dixon and Ekstrand, 1982). However, in addition to the poor manufacturing quality of the diodes, they were very prone to radiation-induced damage. These drawbacks prevented the diodes from continuous use, and so far, they are not listed in the dosimetry systems recommended for use in radiation processing (ICRU Report 80, 2008; ISO/ASTM 52628, 2013). It has been true for any active dosimeter types based on gaseous ionization chambers, diodes (Gonçalves et al., 2024), transistors (Cayley et al., 2024), diamond (Damulira et al., 2019), and recently silica optical fibers (Zubair et al., 2020), many of which are well-established for dosimetry of radiation therapy with high-energy electron beams.

The increasing use of EB accelerators in emerging radiation processing applications, such as biodegradable composites based on bio-renewable resources, industrial wastewater treatment, and human tissue sterilization, continues to drive demand for complementary dosimetry systems and enhance the performance of existing dosimeters. Significant efforts have been made to develop reliable dosimeters that are resistant to radiation damage, with the capability for prompt readout, good spatial resolution, ease of handling, and reasonable cost-effectiveness. Research has been conducted on new luminescent materials to develop thermoluminescent (TL) and optically stimulated luminescent (OSL) dosimeters, which, despite being passive, feature special characteristics for high-dose dosimetry (Asfora et al., 2021; Ley et al., 2020, 2021). The greatest interest lies in new OSL materials due to their simpler and faster readout system compared to TL dosimeters. Recent successful investigations on the effect of high-dose electron beams on pure silica optical fibers, focusing on both the radioluminescence (RL) and radiation-induced attenuation (RIA) phenomena, are reported in the literature (Oresegun et al., 2021). The results demonstrate the potential for real-time use of these silica optical fibers for dose measurements up to 70 kGy in individual exposures, reaching an accumulated dose of almost 300 kGy. The overall promising data obtained so far with these silica optical fibers show the feasibility of their use in EB processing dosimetry, competitively with the diode-based dosimetry system investigated herein.

It is worth noting that the novelty of using diodes as active dosimeters primarily arises from advancements in manufacturing techniques for thin optical devices and radiation hard diodes at very affordable prices (Bueno et al., 2022). This has sparked renewed interest in utilizing them as real-time dosimeters in large-scale industrial processing applications, which had been previously explored in the early days of the radiation processing field.

The online response of active dosimeters based on thin photodiodes has been investigated in an industrial electron beam accelerator covering the dose rate range of 2–8 kGy/s (Gonçalves et al., 2021). The previous results, assessed with the unbiased diode operating in the short-circuit current mode, revealed a linear dose-response with a constant charge sensitivity and stable current signals with repeatability better than 2 %. Such great repeatability enabled the beam dimensions, the background current, and the region corresponding to electrons scattered outside the scan window to be preliminarily identified. In line with these previous findings, this work aims to characterize a 1.5 MeV electron beam irradiator using this homemade diode-based dosimetry system. To take advantage of the proven online diode dosimeter performance, the investigation shall be focused on the relevant operating parameters for routine process control: dose per pass and beam length. To ensure completeness and benchmark these operating parameters for routine process control, gathered in dynamic irradiation mode, alanine and CTA dosimeters, standard passive dosimeters for radiation processing dosimetry, are used.

2. Materials and methods

2.1. Electron beam facility

A Dynamitron DC 1500/25/04 type electron beam accelerator (EBA–model JOB 188), manufactured by Radiation Dynamics, Inc. (currently IBA Industrial), is used in this work. Dosimetry calibrations and the relevant features of this EB facility were previously performed (Kuntz et al., 2015) in terms of Operational Qualification (OQ), according to ISO/ASTM 51649 (2015) and ISO11137-3 (2017). The main technical specifications of the EB accelerator are presented in Table 1. With regards to the dosimetry qualification, previously accomplished with standard reference alanine dosimeters, with traceability to the National Physical Laboratory, radiochromic dosimeters (GEX, FWT), and cellulose triacetate (CTA) films, the main parameters are: electron energy (1.43 MeV), spot size (beam length on the scan window) of 2.54 cm, scan width of 1.02 m with surface dose uniformity better than 6.2 % (k = 2). The dose per pass values under conveyor velocities ranging from 2 to 6 m/min and electron beam current of 1.0 mA are given in Table 2.

2.2. Diode-based dosimetry probe

The batch uniformity of 10 photodiodes (SFH206k supplied by Osram®), (230 ± 5) μm thick and 7.0 mm^2 sensitive area, is verified through the I x V curves, covering the reverse voltage range of (0–30 V). At room temperature (23 °C), all devices exhibit low dark currents spanning from 0.2 nA (0 V) a 1.5 nA (30 V) with variations less than 5 %. The dosimetry probe comprises a light-tight PMMA cylinder (9 mm in diameter and 45 mm in length) with a miniature coaxial connector with a push-pull self-latching system (Lemo®). All current measurements are acquired in the short-circuit mode, with the diode unbiased. The front p^+ pad of each diode is directly connected to the input of a Keithley 6517 B electrometer, while the rear n^+ electrode is grounded through the conducting shield of a coax cable. The electrometer is configured as an amp-meter with the speed of one power line cycle and a range set at 200 μA. In this range, an offset adjustment (zero correct) is performed to minimize the input bias (offset) current to 5 nA and voltage burden less than 100 μV, leading to an accuracy of (0.1 % of reading + 5 nA). Unless otherwise stated, the current signals are acquired under an A/D converter integration time of 0.1 s. For analysis, the current data from the electrometer are directly sent to a computer via a GPIB interface controlled by software developed in LabView.

Table 1
Technical characteristics and the most relevant dosimetry features of the EB facility.

Specifications	Description/Value
Accelerator type	Direct current (DC)
Beam energy	0.5–1.5 MeV
Beam current	0.3–25 mA
Beam power	37.5 kW
Scanning mode	Electromagnetic
Scan frequency	100 Hz
Beam width	60–120 cm
Beam length on window surface	2.54 cm

Table 2
– Doses received by the diode in one pass through the irradiation zone at 4 kGy/s over a conveyor speed range of 2–6 m/min.

Conveyor speed (m/min)	Beam current (mA)	Dose rate (kGy/s)	Dose per pass (kGy)
2	1.0	4	3.0
3	1.0	4	2.0
4	1.0	4	1.5
5	1.0	4	1.2
6	1.0	4	1.0

2.3. Irradiation setup

To replicate the experimental conditions of most irradiation processing applications in this EB facility, all dosimeter types are mounted on a fixture with a backing wood plate (2 cm thick) to prevent them from the backscattered electrons contribution. Each dosimeter fixture is reproducibly mounted onto a conveyor 40 cm away from the center of the beam length. When the movement starts, the dosimeter crosses the irradiation zone along the travel direction and at 17 cm from the scan window.

All irradiations are performed at a constant dose rate (4 kGy/s) and conveyor speeds ranging from 2 to 6 m/min.

For clarity, a schematic diagram of the experimental setup is shown in Fig. 1, where details of the EB facility and the diode-based dosimetry system are given. To help the reader, a diagram showing the beam length, i.e., the dimension of the irradiation zone along the travel direction, and the beam width using a conveyor system is depicted at the top right of Fig. 1. The beam width, or scan width when the beam is electromagnetically scanned, is the dimension of the irradiation zone measured along the scanning direction and, thus, perpendicular to the dosimeter movement. Both beam length and width are set at a specific distance (17 cm) from the scan window (ISO/ASTM 51649, 2015).

2.4. Dose per pass of the EB facility

Irradiations are performed at a constant dose rate (4 kGy/s) and integration time of (0.1 s), with conveyor speeds ranging from 2 to 6 m/min. At each speed, the current signals delivered by the diode during three consecutive passes through the irradiation zone are recorded. The averaged current signal is offline integrated, and the resulting charge is converted to a dose through the calibration curve previously assessed at the same setup under identical experimental conditions (Gonçalves et al., 2021).

The influence of the A/D converter integration time on the current signal shape, and possibly on the dose per pass, is also investigated by acquiring several current signals at different integration times (0.05, 0.1, and 0.55 s) and conveyor velocities (2–6 m/min).

The dose per pass results are benchmarked against those measured with the reference standard alanine dosimeter irradiated at the same position of the diode and experimental parameters of the EB facility as described in section 2.3.

2.5. Beam length of the scanned beam

The experimental approach adopted to measure the beam length with an unbiased diode operating in short-circuit mode relies on the proportionality between the dose rate and the current continuously delivered by the diode during its movement through the irradiation zone. Therefore, the current signal experimentally traduces the dose rate variations as a function of the time while the diode passes through the beam. At a known conveyor velocity, the time is converted to length, and the current or dose rate profile can be used to determine the beam length. The current profile is expected to follow a Gaussian distribution with a maximum current achieved when the diode is exactly underneath the center of the beam length on the scan window surface, known as beam spot size (2.54 cm). The beam length is defined by the full width at half maximum (FWHM) of this Gaussian distribution at a specific distance from the scan window (ISO 51649, 2015).

Beam length measurements are also accomplished with CTA film and alanine dosimeters to validate the proposed method and the results obtained with the diode dosimeter. The experimental setup and details of the dose measurements with CTA and alanine dosimeters are described in the two following sections.

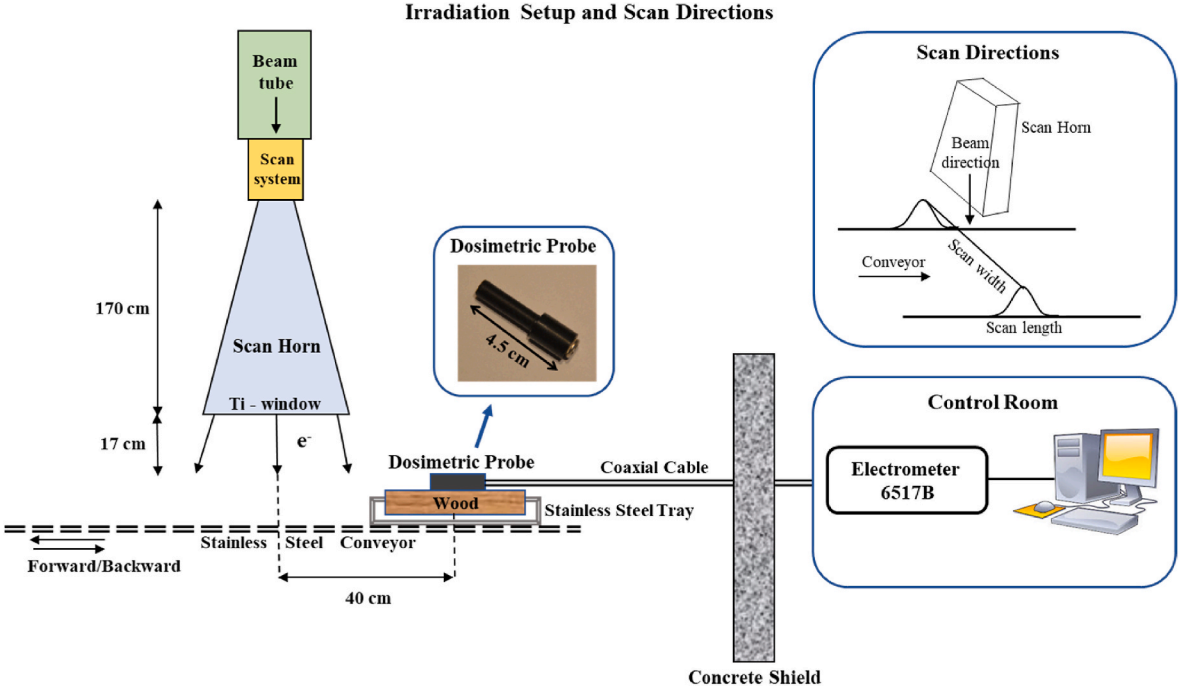

Fig. 1. Schematic diagram of the experimental setup (side view) and scan directions related to the scanned beam using a conveyor system (at the top right).

2.6. Alanine dosimeters

2.6.1. Dose per pass

Dose per pass measurements are carried out with alanine pellets composed of 93 % alanine and 7 % binder (Aerial, France) with 4.0 mm in diameter and 2.2 mm in height settled on an acrylic phantom mounted on the conveyor. The phantom positioning (17 cm from the scan window), dose rate (4 kGy/s), and conveyor speed range (2–6 m/min) are identical to those used for the diode assembly. At each conveyor speed, three pellets are irradiated in several passes through the irradiation field to accumulate a dose (almost 20 kGy) within the alanine operational dose range. The electron spin resonance spectra of the irradiated pellets are acquired with an MS400 ESR spectrometer (Magnettech, Berlin) equipped with the AerEDE dosimetry software (Aerial, France). The spectrometer parameters are set as follows: microwave power of 8 mW, magnetic field centered at 3370 G with field sweep of 30 G, ten scans lasting 12 s each, a gain of 100, and 180° phase. A reference alanine dosimeter is measured at the start and end of readings to ensure the spectrometer's stability. The readouts are converted to dose through an alanine calibration curve earlier attained under the same conditions specific to the irradiator, ESR spectrometer, and dosimeter type (ISO/ASTM 51607, 2013). The average absorbed dose in the three samples is then divided by the number of passes to calculate the dose per pass for each speed.

2.6.2. Beam length

It is measured by statically irradiating ninety alanine pellets settled on an acrylic phantom (20 cm long, 2 cm wide, and 1 cm high) designed with three columns with 30 pellets each. The distance between two alanine centers is 6.5 mm. The longest side of the phantom is oriented along the beam length, which is perpendicular to the beam width. The whole set of alanine, distant 17 cm from the scan window, is irradiated to almost 20 kGy. The average readings of each set of three pellets are plotted against their distance from the center of the phantom, which aligns with the center of the beam width. The electron spin resonance spectra are acquired with the MS400 ESR spectrometer (Magnettech, Berlin) with identical spectrometer parameters described in 2.6.1.

2.7. CTA dosimeter

2.7.1. Beam width

The CTA film is a passive reference dosimeter recommended for assessing the beam length and beam width of EB facilities due to its high spatial resolution (ISO 51650, 2013). In this work, the CTA dosimeter, composed of a 30 cm long film (Fujifilm Radiation Film FTR-125), is fixed on a wooden bar, positioned 17 cm from the scan window. The setup is placed at the center of the radiation field produced by scanning EB and is statically irradiated at 20 kGy. The radiation-induced increase in absorbance of the CTA is measured at a peak wavelength of 280 nm using a DosASAP spectrophotometer (Aerial, France). The spectrometer is controlled by AerODE software (Aerial, France), which automatically sets the measuring parameters, including absorbance mode, wavelength, zero of absorbance, and zero. This software also allows for continuous dose measurements via a serial interface, capturing the absorbance readings and thickness of the film in real time. The specific absorbances, calculated with a maximum uncertainty of 2.5 %, are converted to dose values using a spectrophotometer-specific calibration curve previously established by ISO/ASTM 51261 (2013).

2.8. Overall uncertainties and compliance with standard protocols for radiation processing dosimetry

The technical procedures adopted for measuring the dose per pass and beam length operating parameters of the EB facility are bound to comply with internationally acceptable recommendations for routine dosimetry systems used in radiation processing (ISO/ASTM 51707, 2015) and those specifically addressed for alanine (ISO/ASTM 51607, 2013) and CTA film (ISO 51650, 2013).

An exception is the protocol (IEC 61674, 2024), specifically addressed for diode-based dosimeters in medical dosimetry due to the lack of similar standard protocols for radiation processing.

The combined uncertainties of the experimental results are assessed by adding all the components (types A and B) of the standard uncertainties in quadrature (JCGM, 2008; ISO/ASTM 51707, 2015). The corresponding expanded uncertainty is calculated with a coverage factor $k = 2$, providing a confidence level of about 95 %. The uncertainties budget of the measurements is shown in Table 3.

3. Results and discussion

3.1. Dose per pass

Fig. 2 depicts the current signals delivered by the diode while it is conveyed towards the irradiation zone at varying velocities. All signal profiles are well-fitted by Gaussian functions with similar maximum current values, regardless of the conveyor velocity. These results corroborate the proportionality between current and dose-rate and the good repeatability of the current signals. The repeatability parameter, given by the coefficient of variation (the percentual ratio of the standard deviation to the average value) of these peak current values, is better than 2 %. This result fully supports the IEC 61674 (2024) recommendations.

The influence of the conveyor velocity (v) on the Gaussian current signals is evidenced in Fig. 3, where the full width at half maximum (FWHM) and centroid positioning values are plotted as a function of 1/v. As expected, both data sets are well-fitted by linear functions with R^2 better than 0.9998. The slope of the centroid x 1/v plot, (39.9 ± 0.6) cm, is in good agreement with the distance traveled by the diode from its resting position to the center of the beam length on the scan window surface.

Regardless of the conveyor velocity, the data shown in Figs. 2 and 3 endorses the Gaussian distribution of the current readings during the diode movement and the maximum current delivered when it passes underneath the scan window. Both features are essential to validate the experimental approach to assess the scanned electron beam profile online and the dose per pass.

Measurements of the dose per pass as a function of 1/v, performed at 4 kGy/s and 0.1 s integration time, are shown in Fig. 4. The absorbed dose in each pass of the diode through the beam is inversely proportional to the conveyor speed within the range of 2–6 m/min. These results are benchmarked against those from reference standard alanine dosimeters measured at the same position, dose rate, and conveyor velocity range set up for the diode irradiation.

The agreement between both data sets, within the expanded uncertainty (7.2 %, $k = 2$), corroborates the reliable dose response of this diode-based dosimetry system irradiated under constant dose rate (4 kGy/s), integration time (0.1 s), dose rate (4 kGy/s), and conveyor speed range (2–6 m/min).

The integration time effect on the current signal profile, and possibly the dose per pass, is investigated considering the need for commitment between integration times and conveyor velocities. Ideally, the

Table 3
Uncertainty budget of the dose per pass data.

Component of uncertainty	Value	Type
Calibration doses from laboratory certificate	3.1 %	B
Diode repeatability	1 %	A
Electrometer	0.5 %	B
Conveyor speed	1.5 %	B
Combined uncertainty	3.6 %	
Expanded uncertainty (k = 2)	7.2 %	

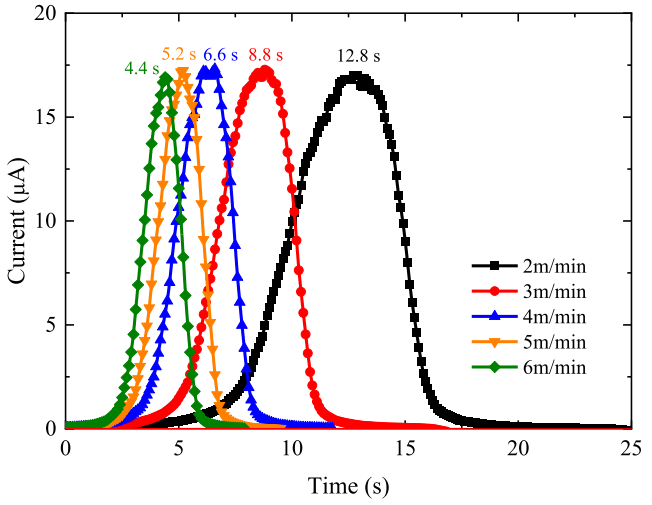

Fig. 2. Current signals recorded at 4 kGy/s while the diode moves through the irradiation zone at varying speeds. The integration time of the electrometer is set at 0.1 s. The centroid values from the Gaussian fitting are displayed just above the peak of each current signal.

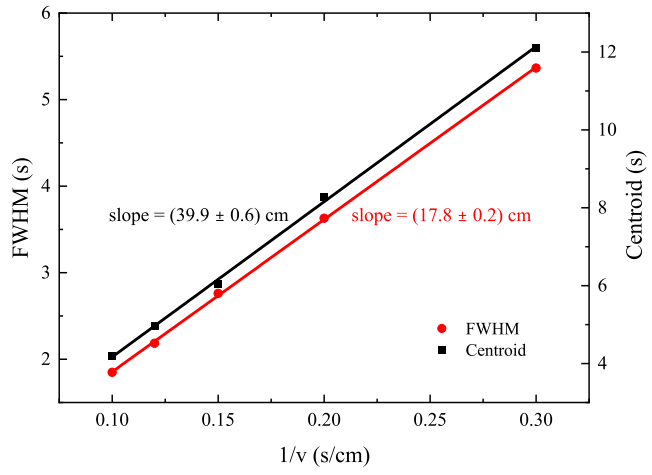

Fig. 3. Centroid and resolution (FWHM) values from Gaussian fittings of the current signals as a function of 1/v. Uncertainties of both slopes arise from the data fittings.

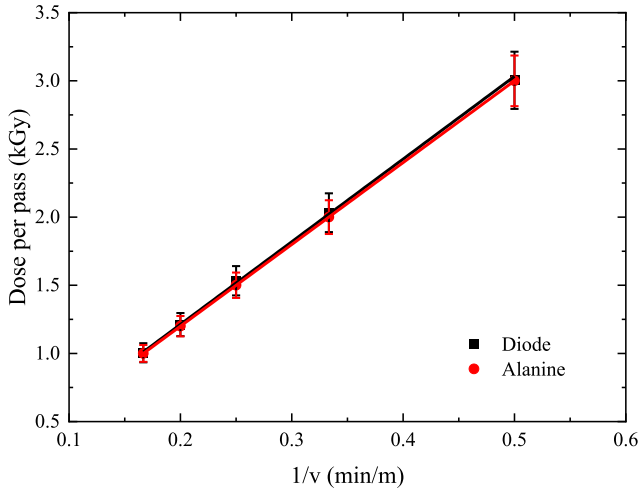

Fig. 4. Dose per pass measurements performed with diode and alanine dosimeters at 2–6 m/min speed range. Irradiations are performed at 4 kGy/s and 0.1 s integration time. Both data sets agree within the overall uncertainties (7.2 %, k = 2).

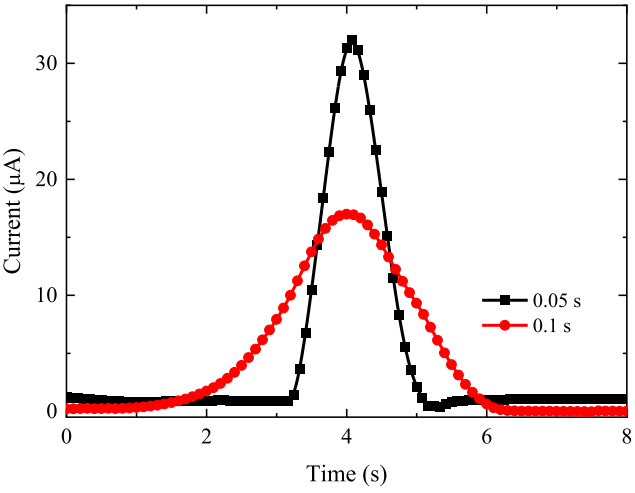

Fig. 5. Current signals assessed with 0.05 s and 0.1 s integration times. Irradiations are performed at 4 kGy/s and 6 m/min conveyor speed.

integration time must be much lower than the traveled distance to the conveyor velocity ratio, i.e., the traveling time of the diode. Measurements are performed with the available integration times of the electrometer (0.05 s, 0.1 s, and 0.55 s) and conveyor velocities from 2 to 6 m/min. Generally, most current signals recorded at a constant integration time under different conveyor speeds are characterized by Gaussian shapes with variable FWHM values. It essentially holds for 0.1 s integration time in the whole velocity range, as evidenced in Fig. 1. The integration time effect on the current signal profile, recorded at 6 m/min, is shown in Fig. 5. Typical Gaussian profiles are achieved with 0.05 s and 0.1 s, both much smaller than the traveling time of the diode. The best temporal resolution (FWHM) is achieved with the fastest integration time, which seems to be the most appropriated for providing

a reliable beam length feature of the EB facility, as described in section 3.2.

On the other hand, the current signal acquired with 0.55 s integration time no longer has a Gaussian profile. As the integration time is almost double the traveling time of the diode (0.25 s), the electrometer starts acting as an integrator of the current readings. It is not a big issue for dose measurements since the integration of the two current signals leads to the same charge and, thus, the same absorbed dose as evidenced in Fig. 6. It shows the overall dose per pass data, assessed through the integration of the current signals recorded at each conveyor velocity and integration time. The dose per pass data acquired with alanine dosimeters are plotted together for comparison and validation purposes.

Fig. 6 evidences a fair matching among the dose values gathered at the same conveyor velocity and different integration times. Additionally, all dose data sets provided by the diode as a function of the conveyor velocity agree with those obtained with alanine dosimeters. This agreement can be quantified by analyzing their residues concerning the dose per pass obtained with the reference standard alanine dosimeters, as presented in Fig. 7.

The overall data is characterized by residues less than 6 %, which validates the reliable dosimetry performance of the diode in the whole velocity and integration time ranges. It is important to note that the lowest residues consistently found in the whole velocity range for an integration time of 0.1 s favor its choice to enhance the dose response of the dosimeter. Furthermore, the residues related to the alanine less than

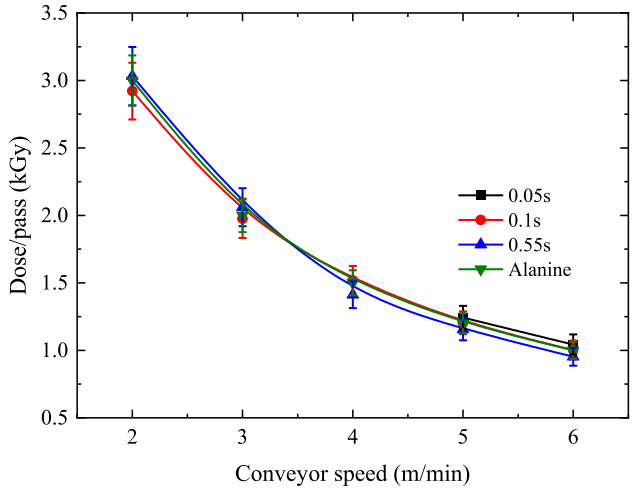

Fig. 6. Dose per pass data obtained with the diode irradiated at 4 kGy/s as a function of the conveyor speed between 2 and 6 m/min and distinct integration times. The dose per pass provided by the reference alanine dosimeter is plotted together with the diode results for comparative purposes.

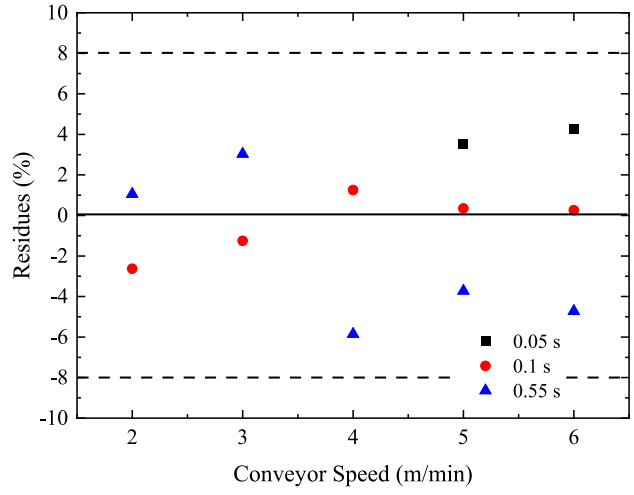

Fig. 7. – Residues of the dose per pass data related to those provided by the reference alanine dosimeters (continuous line at the center of the plot). The dashed lines represent the maximum acceptable variation (8 %, k = 2) in the dosimeter response recommended by ISO/ASTM 51607 (2013).

6 % fully comply with the maximum acceptable variation (8 %, k = 2) in the dosimeter response recommended by ISO/ASTM 51607 (2013).

3.2. Beam length

The assessment of the scanned beam profile, at 17 cm from the scan window, is initially performed with the Gaussian current signals recorded at different velocities (Fig. 2). At a known velocity, the beam profile is obtained by converting the time axis of the current signal to the distance traveled by the diode through the radiation field. As shown in Fig. 8, all beam profiles are characterized by peak current readings when the diode crosses the center of the scan window, 40 cm away from the starting position of its movement along the conveyor direction. This result agrees with the slope of the current signal centroid as a function of 1/v plot, (39.9 ± 0.6) cm, presented in Fig. 3. The FWHM data, obtained through the Gaussian fittings of the beam profiles, is presented in Table 4.

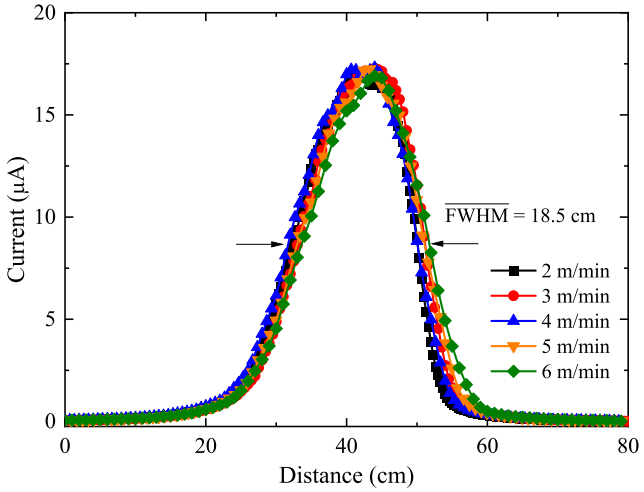

Fig. 8. Expanded view of the current profiles recorded at 4 kGy/s and 0.1 s integration time when the diode crosses the irradiation field with conveyor speeds ranging from 2 m/min to 6 m/min. The agreement among the FWHM values is better than 2 %.

Table 4
– FWHM (cm), beam lenght, at 17 cm from the scan window, 4 kGy/s dose rate and 0.1 s acquisition time.

Conveyor Speed (m/min)	FWHM (s)	FWHM[a] (cm)	FWHM[b] (cm)
2	5.4 ± 0.4	17.9 ± 1.3	18.2 ± 1.3
3	3.6 ± 0.3	18.2 ± 1.3	18.2 ± 1.3
4	2.8 ± 0.2	18.4 ± 1.3	18.6 ± 1.3
5	2.2 ± 0.2	18.2 ± 1.3	18.5 ± 1.3
6	1.9 ± 0.1	18.5 ± 1.3	18.9 ± 1.3
average	–	18.3 ± 1.3	18.5 ± 1.3

[a] FWHM (s) multiplied by each conveyor speed.
[b] FWHM (cm) from the fitting of the scanned beam profiles.

The correspondent average value of (18.5 ± 1.3) cm fully agrees with (17.8 ± 0.2) cm given by the slope of the FWHM x 1/v plot (Fig. 3). These both results regarding centroid position and FWHM of the scanned beam profile, assessed at 17 cm from the scan window and 0.1 s integration time of the electrometer confirm the beam profile independence on the conveyor velocity within the range here investigated.

However, this statement does not hold straightforwardly for 0.05 s and 0.55 s integration time covering the conveyor velocity range. The integration time effect on the current signal profile is evidenced in Fig. 3, where current readings, performed at 6 m/min, 0.05 s and 0.1 s integration times, are plotted together. Both correspondent beam profiles are well fitted by Gaussian function with FWHM slightly favoring the resolution (9.7 ± 0.3) cm for 0.05 s integration time (Fig. 9). It is important to note that, both integration times fulfill the requirement of being much less than the traveling time of the diode under the scan window (0.25 s).

The data provided by the diode (6 m/min and 0.05 s) is benchmarked against those assessed with reference standard alanine and CTA film dosimeters to validate the straightforward approach for assessing the scanned beam profile through the current signals. To allow the direct comparison among the whole data, the normalized response of the two passive dosimeters (related to absorbed dose) and the active diode-based dosimeter (related to current) are presented in Fig. 10. It evidences that all beam profiles are fitted by Gaussian functions, with a perfect matching in the centroid peaks at the center of the scan window as highlighted in the plot. This region is similar to the beam spot size (2.54 cm) or the beam length on the window surface, previously measured in

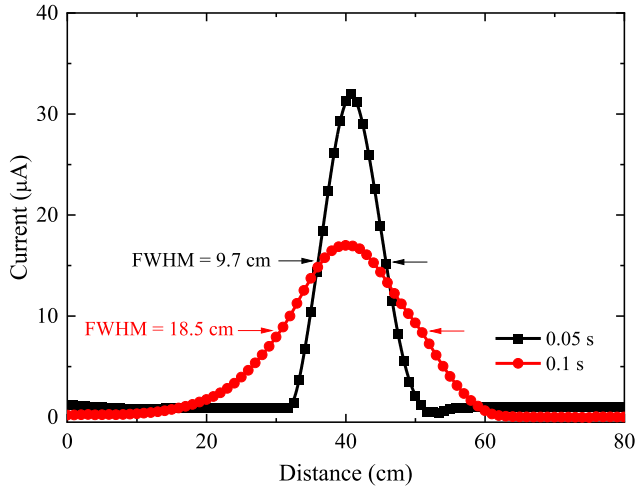

Fig. 9. Current profiles assessed with 0.05 s and 0.1 s integration times. Irradiations are performed at 4 kGy/s and 6 m/min conveyor speed.

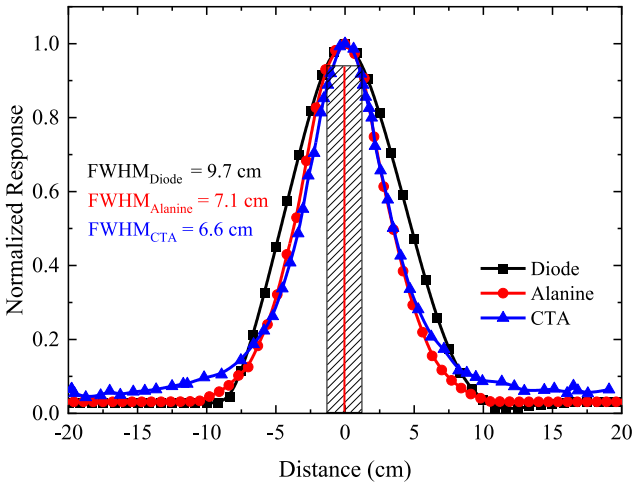

Fig. 10. Expanded view of a current profile recorded at 4 kGy/s and 0.05 s integration time when the diode crosses the irradiation field produced by the scanned beam. The data is benchmarked against those statically measured with alanine and CTA film dosimeters. All irradiations are performed at 17 cm from the scan window.

operational qualifications of the EB facility.

Furthermore, there is a good agreement between the beam profiles statically measured with CTA film and alanine dosimeters, despite their different spatial resolutions. This effect leads to a negligible enlargement (5 mm) in the FWHM provided by the alanine dosimeters. The same volumetric effect explains the broadening of the beam profile (FWHM = 9.7 cm) measured with the diode during its movement through the irradiation field produced by the scanned beam. Another effect that could change the current signal shape and resolution is setting a suitable integration time considering the conveyor velocity and the distance the diode travels underneath the scan window. This issue, inherently linked to dynamic irradiations of active dosimeters and characteristic of the EB facility, is experimentally minimized with an integration time of 0.05 s.

Despite the challenges posed by dynamic irradiations, the small difference in beam profiles measured by the three dosimeters validates the straightforward approach to measure the beam length parameter and the suitability of using the diode for monitoring scanned beam profiles.

4. Conclusions

The results concerning the characterization of an industrial-scale electron beam irradiator using an online diode-based dosimetry system, previously developed and calibrated for routinely monitoring irradiation process, are presented in this work. To take advantage of the diode dosimetry performance with linear dose response and stable current signal proportional to the dose rate, the investigation focused on the relevant operating parameters for routine process control: dose per pass and beam length measurements. The dose per pass results, obtained through integrating the current signals delivered by the diode irradiated at a constant dose rate (4 kGy/s) under (2–6 m/min) conveyor speeds, are fully validated by the data from the reference standard alanine dosimeters. It holds even when the integration times vary from 0.05 to 0.55 s, despite the pronounced effect on the current signal shape, corroborating the necessary commitment between the integration time and the traveling time of the diode through the radiation field produced by the scanned beam. It is worth noting that, for this facility and the conveyor speed range, the most precise dose per pass results, quantified through the lowest residues to the standard alanine measurements, are obtained for 0.1 s. Under this condition, the integration time effect is negligible. All current signals can be fitted by Gaussian functions with centroid and FWHM parameters well defined (Fig. 2). It is essential to the straightforward method proposed in this work to assess the beam length through a current signal that experimentally traduces the dose rate variations as a function of the time while the diode passes through the beam. At a known velocity, the time is converted to length, and the FWHM of the current or dose rate profile provides the beam length measurement at a certain distance from the scan window. The validity of this proposed method is checked by replicating the experimental conditions (4 kGy/s, 6 m/min, and 17 cm from the scan window) used in most routine processes conducted in this EB facility. The integration time effect on the signal profile is again evidenced in the beam length FWHM values measured with 0.05 s (9.7 cm) and 0.1 s (18.5 cm). A comparison among these beam profiles and those FWHM assessed with CTA film (6.6 cm), a standard dosimeter for this type of measurement and alanine dosimeters (7.1 cm) evidences the best agreement found with the narrower one assessed with 0.05 s. Furthermore, the differences between the spatial resolution of the dosimeters perfectly justify the small discrepancies found in the FWHM values.

Finally, it is noteworthy that the overall results presented herein, benchmarked against those assessed with reference standard passive dosimeters for radiation processing dosimetry, not only validate the straightforward approach to measure the dose per pass and beam length parameters, but also endorses the reliable performance of this diode-based system as an inexpensive and reliable dosimeter for routine process control.

CRediT authorship contribution statement

J.A.C. Gonçalves: Writing – review & editing, Resources, Methodology, Investigation, Formal analysis, Data curation. **V.K. Asfora:** Investigation, Data curation. **H.J. Khoury:** Writing – review & editing, Funding acquisition. **C.C. Bueno:** Writing – review & editing, Writing – original draft, Supervision, Methodology, Formal analysis, Conceptualization.

Declaration of competing interest

The authors declare that they have no known competing financial interests or personal relationships that could have appeared to influence the work reported in this paper.

Acknowledgments

The authors highly acknowledge the collaboration of Engs. Elizabeth

S. R. Somessari and Vladimir Lepk from the Electron Beam Accelerator staff (IPEN-CNEN/SP) for their indispensable help during irradiation. The authors also thank R. C. Teixeira and N. Carvalho, both from Centro de Tecnologia da Informação Renato Archer (CTI-Renato Archer, Campinas/SP), for the electrical characterization of the diodes. This work is part of the Brazilian Institute of Science and Technology for Nuclear Instrumentation and Applications to Industry and Health (INCT/INAIS), CNPq project 406303/2022–3. FAPESP partially supports this work under contract 2018/05982–0.

Data availability

Data will be made available on request.

References

Asfora, V.K., Antonio, P.L., Gonçalves, J.A.C., Bueno, C.C., de Barros, V.S.M., Oliveira, C. N.P., Caldas, L.V.E., Khoury, H.J., 2021. Evaluation of TL and OSL responses of CaF_2: Tm for electron beam processing dosimetry. Radiat. Meas. 140, 106512. https://doi.org/10.1016/j.radmeas.2020.106512.

Barthe, J., 2001. Electronic dosimeters based on solid-state detectors. Nucl. Instrum. Methods B 184, 158–189. https://doi.org/10.1016/S0168-583X(01)00711-X.

Benny, P.G., Khader, S.A., Sarma, K.S.S., 2014. Evaluation of various operational and dosimetric parameters of an industrial electron beam accelerator of 2 MeV energy. Nucl. Instrum. Methods 751, 88–94.

Bueno, C.C., Camargo, F., Gonçalves, J.A.C., Pascoalino, K., Mangiarotti, A., Tuominen, E., Härkönen, J., 2022. Performance characterization of dosimeters based on radiation-hard silicon diodes in gamma radiation processing. Front. Sens. 3, 770482. https://doi.org/10.3389/fsens.2022.770482.

Calvo, W.A.P., Duarte, C.L., Machado, L.D.B., Manzoli, J.E., Geraldo, A.B.C., Kodama, Y., Silva, L.G.A., Pino, E.S., Somessari, E.S.R., Silveira, C.G., Rela, P.R., 2012. Electron beam accelerators - trends in radiation processing technology for industrial and environmental applications in Latin America and the Caribbean. Radiat. Phys. Chem. 81, 1276–1281. https://doi.org/10.1016/j.radphyschem.2012.02.013.

Cayley, J., Tan, Y.-R.E., Petasecca, M., Cutajar, D., Breslin, T., Rosenfeld, A., Lerch, M., 2024. MOSkin dosimetry for an ultra-high dose-rate, very high-energy electron irradiation environment at PEER. Front. Phys. 12, 1401834. https://doi.org/10.3389/fphy.2024.1401834.

Chilkulwar, R.H., Sharma, S.D., Chaudhary, N., Acharya, S., Mayya, Y.S., Mittal, K.C., Gantayet, L.M., 2012. Dosimetric evaluation of an indigenously developed 10 MeV industrial electron beam irradiator. Radiat. Meas. 47, 628–633. https://doi.org/10.1016/j.radmeas.2012.06.009.

Cleland, M.R., Thompson, C.C., Saito, H., Lisanti, T.F., Burgess, R.G., Malone, H.F., Loby, R.J., Galloway, R.A., 1993. New high-current Dynamitron accelerators for electron beam processing. Nucl. Instrum. Methods Res. B 79, 861–864. https://doi.org/10.1016/0168-583X(93)95486-O.

Cleland, M.R., Parks, L.A., Cheng, S., 2003. Applications for radiation processing of materials. Nucl. Instrum. Methods Phys. Res. B. 208, 66–73. https://doi.org/10.1016/S0168-583X(03)00655-4.

Cleland, M.R., 2006. Industrial Applications of Electron Accelerators. CAS - CERN Accelerator School and KVI: Specialised CAS Course on Small Accelerators, The Netherlands. https://doi.org/10.5170/CERN-2006-012.383. Zeegse 24 May - 2 Jun 2005, 383-416 (CERN-2006-012).

Damulira, E., Yusoff, M.N.S., Omar, A.F., Taib, N.H.M., 2019. A review: photonic devices used for dosimetry in medical radiation. Sensors 19, 2226–2254. https://doi.org/10.3390/s19102226.

Dixon, R.L., Ekstrand, K.E., 1982. Silicon diode dosimetry. Int. J. Appl. Radiat. Isot. 33, 1171–1176.

Farah, K., Kuntz, F., Kadri, O., Ghedira, L., 2004. Investigation of the effect of some irradiation parameters on the response of various types of dosimeters to electron irradiation. Radiat. Phys. Chem. 71, 337–341. https://doi.org/10.1016/j.radphyschem.2004.02.041.

Galloway, R.A., DeNeuter, S., Lisanti, T.F., Cleland, M.R., 2004a. The new IBA self-shielded dynamitron accelerator for industrial applications. Radiat. Phys. Chem. 71, 281–283. https://doi.org/10.1016/j.radphyschem.2004.03.060.

Galloway, R.A., Lisanti, T.F., Cleland, M.R., 2004b. A new 5 MeV-300kW dynamitron for radiation processing. Radiat. Phys. Chem. 71, 549–551. https://doi.org/10.1016/j.radphyschem.2004.03.059.

Gonçalves, J.A.C., Mangiarotti, A., Asfora, V.K., Khoury, H.J., Bueno, C.C., 2021. The response of low-cost photodiodes for dosimetry in electron beam processing. Rad. Phys. and Chem. 181, 109335–109342. https://doi.org/10.1016/j.radphyschem.2020.109335.

Gonçalves, J.A.C., Mangiarotti, A., Antonio, P.L., Caldas, L.V.E., Bueno, C.C., 2024. Dosimetric parameters and radiation tolerance of epitaxial diodes for diagnostic radiology and computed tomography beams. Radiat. Phys. Chem. 223, 111926. https://doi.org/10.1016/j.radphyschem.2024.111926.

IAEA TECDOC-2008, 2022. International Atomic Energy Agency, Development of Electron Beam and X Ray Applications for Food Irradiation. IAEA, Vienna.

IEC 61674, 2024. Medical Electrical Equipment - Dosimeters with Ionization Chambers And/or Semiconductor Detectors as Used in X-Ray Diagnostic Imaging, third ed. 2024.

ISO/ASTM 51261, 2013. Practice for Calibration of Routine Dosimetry Systems for Radiation Processing. https://doi.org/10.1520/ISOASTM51261-04, 2nd ed., 2013.

ISO/ASTM 51607, 2013. Practice for Use of the Alanine-EPR Dosimetry System, third ed. https://doi.org/10.1520/ISOASTM51607-13 2013.

ISO/ASTM 51650, 2013. Practice for Use of a Cellulose Triacetate Dosimetry System. https://doi.org/10.1520/ISOASTM51650-13, 2013.

ISO/ASTM 52628, 2013. Standard Practice for Dosimetry in Radiation Processing, first ed. https://doi.org/10.1520/ISOASTM52628-13 2013.

ISO/ASTM 51649, 2015. Practice for Dosimetry in an Electron Beam Facility for Radiation Processing at Energies between 300 keV and 25 MeV, third ed. https://doi.org/10.1520/ISOASTM51649-15 2015.

ISO/ASTM 51707, 2015. Standard Guide for Estimation of Measurement Uncertainty in Dosimetry for Radiation Processing, third ed. https://doi.org/10.1520/ISOASTM51707-15 2015.

ISO/ASTM 11137-3, 2017. Sterilization of health care products - radiation Part 3: guidance on dosimetric aspects of development. Validation and Routine Contro, second ed. l 2017.

JCGM 100, 2008. Evaluation of measurement data – guide to the expression of uncertainty in measurements (GUM 1995 with minor corrections). Available free of charge at the BIPM website. http://www.bipm.org.

Kneeland, D.R., Nablo, S.V., Weiss, D.E., Sinz, T.E., 1999. Industrial use of the real-time monitor for quality assurance in electron processing. Radiat. Phys. Chem. 55, 429–436. https://doi.org/10.1016/S0969-806X(99)00190-5.

Kuntz, F., Somessari, E.S.R., da Silveira, C.G., Bueno, C.C., Calvo, W.A.P., Napolitano, C. M., Gonçalves, J.A.C., Somessari, S.L., 2015. A dosimetric survey of the DC1500/25/04 electron beam plant installed at IPEN-CNEN/SP. In: Proceedings 2015 International Nuclear Atlantic Conference. São Paulo, Brazil, 978-85-99141-06-9.

Ley, K., Hashim, S.A., Lohstroh, A., Shenton-Taylor, C., Bradley, D.A., 2020. Thermoluminescent response of silica beads to high-dose irradiations. Radiat. Phys. Chem. 167, 108349. https://doi.org/10.1016/j.radphyschem.2019.108349.

Ley, K., Hashim, S.A., Lohstroh, A., Shenton-Taylor, C., Bradley, D.A., 2021. Fading and residual responses for thermoluminescent dosimetry of silica beads irradiated using a high-dose electron-beam. Radiat. Phys. Chem. 182, 109366. https://doi.org/10.1016/j.radphyschem.2021.109366.

McLaughlin, W.L., Boyd, A.W., Chadwick, K.H., McDonald, J.C., Miller, A., 1989. Dosimetry for Radiation Processing. Taylor & Francis (Hemisphere Publishing Corporation), Basingstoke, Hampshire, UK, p. 264, 19890-85066-740-2.

Möhlmann, J.H.F., 1981. The use of solar cells for continuous recording of absorbed dose in the product during radiation sterilization. In: Biomedical Dosimetry, Proceedings of Symposium, Vienna, 1981. IAEA Publication STI/PUB/567, p. 563.

Muller, A.C., 1970a. The "n" on "p" solar-cell dose-rate meter. In: Holm, N.W., Berry, R.J. (Eds.), Manual on Radiation Dosimetry, p. 423. New York.

Muller, A.C., 1970b. The "p" on "n" solar-cell integrating dosimeter. In: Holm, N.W., Berry, R.J. (Eds.), Manual on Radiation Dosimetry, p. 429. New York.

Oresegun, A., Zubair, H.T., Ghassan, L., Abdul-Rashid, H.A., Hashim, S.A., Bradley, D.A., 2021. Effects of hydroxyl content in pure silica optical fiber exposed to kGy electron beams. Radiat. Phys. Chem. 178, 108975. https://doi.org/10.1016/j.radphyschem.2020.108975.

Osvay, M., Stenger, V., Földiak, G., 1975a. Silicon detectors for measurement of high exposure rate gamma rays. In: Biomedical Dosimetry, Proceedings of Symposium. IAEA Publication STI/PUB/401, Vienna, 1974, p. 623.

Osvay, M., Tárczy, K., 1975b. Measurement of γ-dose rates by n- and p-type semiconductor detectors. Phys. Stat. Sol. 27 (A), 285–290.

Smith, M., Galloway, R., 2004. Evaluation of in-line electron beam system requirements and capabilities. Radiat. Phys. Chem. 71, 529–530. https://doi.org/10.1016/j.radphyschem.2004.03.053.

Yuan, J., Zhang, G., Pang, S., Chen, T., Huang, J., 2023. Study and design of an energy monitoring device for an industrial electron accelerator using Monte Carlo simulation. Radiat. Phys. Chem. 206, 110808–110814. https://doi.org/10.1016/j.radphyschem.2023.110808.

Zubair, H.T., et al., 2020. Recent advances in silica glass optical fiber for dosimetry applications. IEEE Photon. J. 12 (3), 6801525. https://doi.org/10.1109/jphot.2020.2985857.